Sensors and Actuators B 266 (2018) 302–310

Contents lists available at ScienceDirect

Sensors and Actuators B: Chemical

journal homepage: www.elsevier.com/locate/snb

Enhanced gas sensing properties of monodisperse Zn_2SnO_4 octahedron functionalized by PdO nanoparticals

Xueli Yang, Hongyu Gao, Liupeng Zhao, Tianshuang Wang, Peng Sun*, Fangmeng Liu, Geyu Lu*

Jilin University, 2699 Qianjin Street, Changchun 130012, China

ARTICLE INFO

Article history:
Received 31 October 2017
Received in revised form 6 February 2018
Accepted 19 March 2018
Available online 20 March 2018

Keywords:
Zn_2SnO_4 octahedron
PdO nanoparticles
Hydrothermal method
Gas sensor

ABSTRACT

In this work, Zn_2SnO_4 microstructures functionalized with PdO nanoparticles were successfully synthesized combination a facile one-step hydrothermal method and subsequent wet impregnation treatment. X-ray diffraction (XRD), field-emission scanning electron microscopy (FESEM), transmission electron microscopy (TEM), and selected-area electron diffraction (SAED) were employed to obtain the crystalline and morphological characterization of the as-prepared products. The results demonstrated that the morphology of the final Zn_2SnO_4 samples have uniform octahedral structure. Interestingly, the surface of Zn_2SnO_4 octahedrons was assembled by nanosheets with the assistant of CTAB. In addition, gas-sensing properties of the as-prepared Zn_2SnO_4 octahedrons before and after functionalization with PdO nanoparticles were systematically investigated. Compared with pure Zn_2SnO_4, the sensor based on 2 wt% PdO-loaded Zn_2SnO_4 octahedrons exhibited obviously enhanced gas sensing properties toward ethanol. The response value was 82.3 toward 100 ppm ethanol, which was almost five times higher than that of pure Zn_2SnO_4. The novel structure of Zn_2SnO_4 octahedrons and the catalytic effect of PdO nanoparticles were believed to be the main reason of the enhancement of gas sensing characteristics.

1. Introduction

During the past decades, gas sensors based on oxide semiconductors have been extensively investigated due to their excellent sensitivity, and have found use in monitoring and detecting pollutants, combustible and toxic gases [1–3]. Previous researches have showed that the gas sensing properties of oxide semiconductors were closely related with their composition, crystalline size, and surface morphology. Therefore, various kinds of metal oxide semiconductors with different microstructures and morphologies have been prepared and applied in gas sensors, due to their unique advantages, including low cost, easy synthesis, and high response [4–18]. Although remarkable achievement has been made in fabricating gas sensors, the development of new sensors strategies for ever increasing sensitivity, selectivity, response and recovery rate still remains one of the major scientific challenges.

Zinc stannate (Zn_2SnO_4) is an important *n*-type ternary semiconductor oxide with a wide band gap of 3.6 eV. Zn_2SnO_4 has cubic inverse spinel structure with high electrical conductivity, high electron mobility, low visible absorption, as well as high chemical sensitivity. Because of its excellent properties Zn_2SnO_4 recently attracted considerable research interests in many promising applications, such as photocatalyst [19–21], solar cells [22–24], anode material for Li-ion batteries [25–27], and gas sensors [28–30]. Many studies have been conducted in order to improve the performance of Zn_2SnO_4 gas sensors, however, these studies were mainly focused on the constructing of novel structures [31–33]. Noble metal loading could improve the gas sensing performance of semiconductor oxides, and related literatures have been reported. Above all the reported literature about Zn_2SnO_4 materials on gas sensors, there is no report of noble metal loading on Zn_2SnO_4 materials to improve the sensing performance. Therefore, it is necessary to design and fabricate high performance gas sensor based on Zn_2SnO_4 with PdO loading.

In this paper, pure and PdO-loaded Zn_2SnO_4 octahedrons decorated with nanosheets were successfully synthesized via a facile hydrothermal route combined with subsequent impregnation treatment. A comparative investigation of sensing properties reveal that the sensing performance of PdO-functionalized Zn_2SnO_4 octahedrons exhibited dramatic improvement in response toward ethanol due to the unique architecture and catalytic effect of PdO.

* Corresponding authors.
E-mail addresses: pengsun@jlu.edu.cn (P. Sun), lugy@jlu.edu.cn (G. Lu).

https://doi.org/10.1016/j.snb.2018.03.121
0925-4005/

Our work is an exploratory research that will provide reference for future research.

2. Experimental section

2.1. Synthesis process

2.1.1. Synthesis of Zn2SnO4 octahedrons

All of the chemical reagents involved in the experiment were of analytical grade and were used as received without further purification. In a typical process, 1 mmol of zinc sulfate heptahydrate ($ZnSO_4{\cdot}7H_2O$) and 0.5 mmol of tin chloride pentahydrate ($SnCl_4{\cdot}5H_2O$) were dissolved in 40 mL of deionized water, after magnetic stirring for about 20 min. 0.08 g of CTAB and 6 mmol of NaOH were added into the above mixed solution and continued stirring for about 30 min. The homogeneous solution was transferred into a 50 mL of Teflon-lined stainless steel autoclave that was then sealed, maintained at 200 °C for 24 h. Subsequently the autoclave was allowed to cool down to room temperature naturally. The resulting precipitates were collected by centrifugation and washed several times with deionized water and ethanol alternately, then dried in air at 80 °C for 12 h. Finally, the nanosheets decorated octahedral Zn_2SnO_4 particles were obtained after annealing at 500 °C for 2 h in air atmosphere with a heating rate of 2 °C/min.

2.1.2. Synthesis of PdO-loaded Zn_2SnO_4 octahedrons

PdO deposition was accomplished by a wet impregnation method, $PdCl_2$ as precursor. Simply, 50 mg of as-prepared Zn_2SnO_4 powders were dissolved in 20 mL of absolute ethanol solvent and then different weight percent of PdO (1 wt%, 2 wt%, and 4%) was dissolved in the above solution, respectively. The slurry was dried at 40 °C, and then calcined at 300 °C for 2 h to obtain the PdO-loaded Zn_2SnO_4 materials.

2.2. Characterization

The X-ray powder diffraction (XRD) pattern of the as prepared samples were performed on a Rigaku D/Max–2550 V X-ray diffractometer using high-intensity Cu-Kα radiation (λ = 1.54178 Å), and the data was collected in the range of 20–80° (2θ) to investigate the crystal structure. The morphology of the as-prepared products was observed by field emission scanning electron microscopy (FESEM) on a JSM-7500F (JEOL) microscope operating at an accelerating voltage of 15 kV. Transmission electron microscopy (TEM) and high-resolution transmission electron microscopy (HRTEM) observations were carried out on a JEM-2200FS apparatus (JEOL) operating at 200 kV. The surface elemental composition was performed with X-ray photoelectron spectroscopy (XPS, Thermo ESCALAB 250XI). All of the binding energies in the XPS analysis were calibrated for specimen charging by reflecting to the signal of carbon C 1s peak with a binding energy of 284.7 eV.

2.3. Fabrication and measurement of gas sensor

The gas sensor was fabricated as follows: the as-prepared Zn_2SnO_4 samples were mixed with deionized water in order to form a homogeneous paste. Subsequently the paste was coated on an alumina tube with the help of a small brush. The alumina tube was about 4 mm in length, 1.2 mm in external diameter, and 0.8 mm in internal diameter. Besides, a pair of Au electrodes was installed on the end of the tube, and each electrode was connected with a pair of Pt wires. After drying in air at room temperature, the device was calcined at 400 °C for 2 h, and then a Ni-Cr alloy coil was inserted into the alumina tube as a heater, allowing us to control the operating temperature of the sensor by adjusting the heating current. The schematic structure of the gas sensor was depicted in Fig. 1. The gas-sensing performance of the sensor was evaluated under laboratory conditions (40RH%, 23 °C). The measurement was processed by a static process: a given amount of the tested gas was injected into a closed glass chamber, and the sensor was put into the chamber for the measurement of the sensitive performance. The response of the sensor was defined as S = Ra/Rg for reducing gas or Rg/Ra for oxidizing gas. The response time and recovery time were defined as the time taken by the sensor to achieve 90% of the total resistance change after the sensor was exposed to the tested gas and air, respectively.

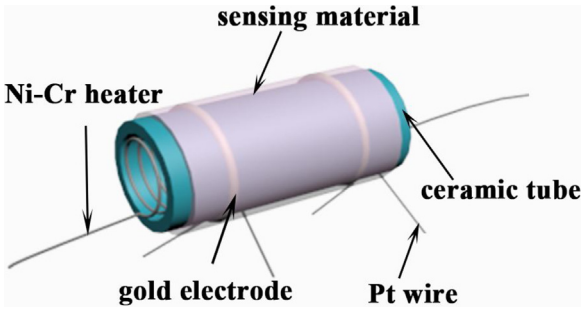

Fig 1. Schematic structure of the gas sensor.

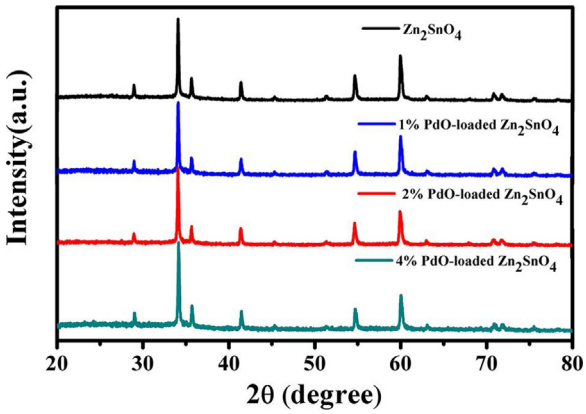

Fig. 2. (a) XRD patterns of the as-prepared composites.

3. Results and discussion

3.1. Structural and morphological characteristics

The composition and crystalline phase of the obtained products were conducted by powder X-ray diffraction (XRD). Fig. 2 shows the XRD patterns of the unloaded and PdO-loaded Zn_2SnO_4 samples. It is clear that all of the observed diffraction peaks of the products were matched well with the pure cubic inverse spinel Zn_2SnO_4, which was in good agreement with the standard JCPDS card of Zn_2SnO_4 (JCPDS 24-1470). However, as for the PdO-loaded Zn_2SnO_4 products, with the variation of loaded PdO nanoparticles, the diffraction peaks could still be indexed to the standard JCPDS card of Zn_2SnO_4 (JCPDS 24-1470), which might be ascribed to the low PdO content compared with Zn_2SnO_4 samples. Furthermore, no other diffraction peaks derived from other phases or possible impurities such as ZnO and SnO_2 were found, indicating high purity of the as-synthesized products.

To further investigate the surface chemical composition and the valence state of the pure and 2 wt% PdO-loaded Zn_2SnO_4 samples, X-Ray photoelectron spectroscopy (XPS) measurements were performed. As shown in Fig. 3a, the full scale XPS spectra showed pure and 2 wt% PdO-loaded Zn_2SnO_4 the samples were mainly com-

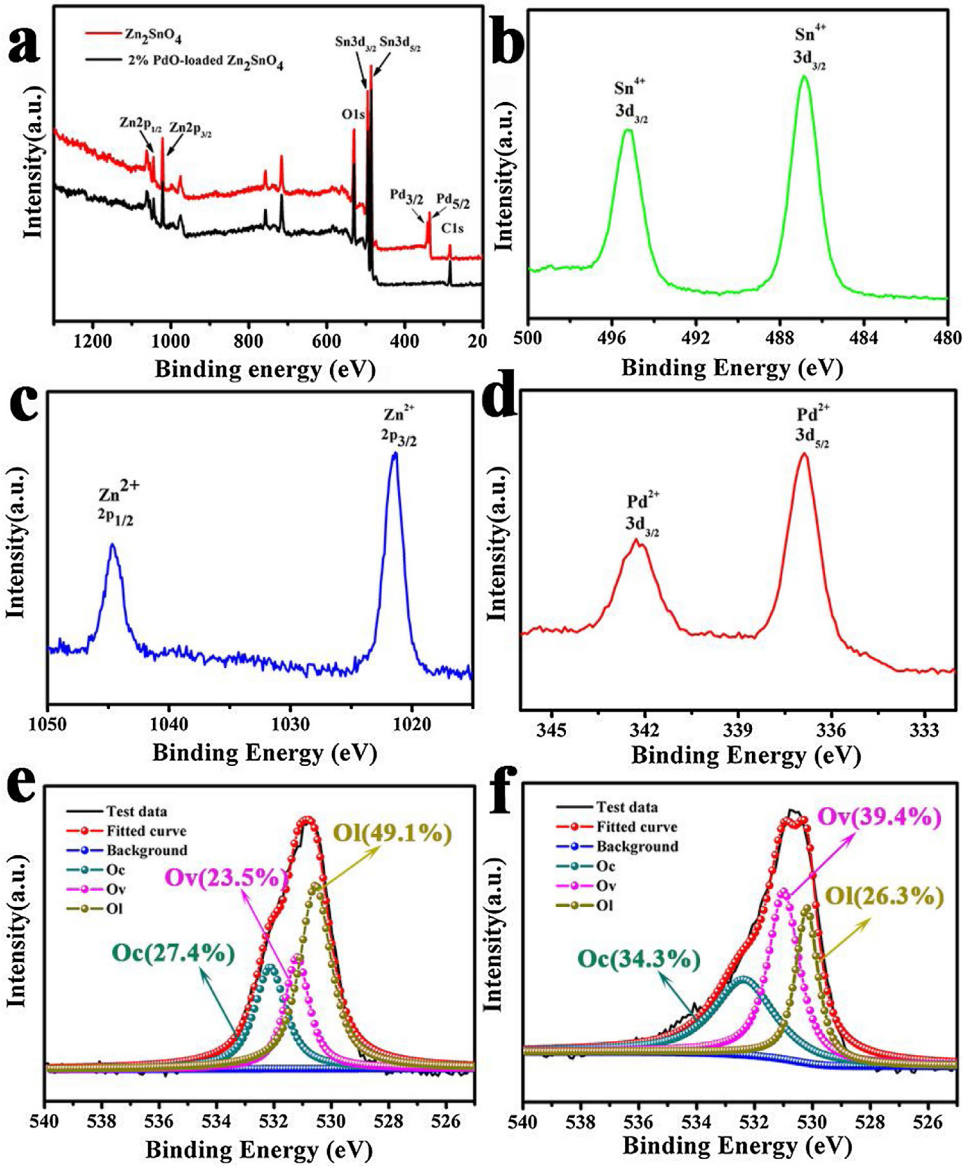

Fig. 3. (a) Wide XPS spectrum of pure and 2 wt% PdO-loaded Zn_2SnO_4 products. (b–d) High resolution XPS spectra of 2 wt% PdO-loaded Zn_2SnO_4:(b) Sn 3d. (c) Zn 2p. (d) Pd 3d. (e–f) O 1 s spectrum of pure (e) and 2 wt% PdO-loaded Zn_2SnO_4 products (f).

posed of Zn, Sn, C, and O, and it is worth noting that the presence of PdO is revealed by the XPS spectrum in 2 wt% PdO-loaded Zn_2SnO_4. Fig. 3b–d exhibited the high resolution XPS spectra of Sn, Zn, and Pd in 2 wt% PdO-loaded Zn_2SnO_4. Two strong peaks centered at 486.9 eV and 495.2 eV can be attributed to the bonding energies of $Sn3d_{5/2}$ and $Sn3d_{3/2}$, respectively, which corresponding to the binding energies of Sn^{4+} states (Fig. 3b). The peaks centered at 1021.3 eV and 1044.6 eV showed in Fig. 1d are assigned to the Zn $2p_{3/2}$ and Zn $2p_{1/2}$ of Zn^{2+} valence state (Fig. 3c). For the chemical state of Pd in the obtained product, the spectrum of Pd-3d had two characteristic peaks with binding energies of about 336.8 eV and 342.2 eV revealed the Pd^{2+} state, which confirms the existence of PdO in the 2 wt% PdO-loaded Zn_2SnO_4 products [34]. Fig. 3e and f depicts the O–1 s spectra of pure and 2 wt% PdO-loaded Zn_2SnO_4, respectively. It can be found that both of the test curves could be decomposed into three oxygen species: the lattice oxygen (O_L), oxygen vacancy (O_v), and chemisorbed oxygen (O_c), respectively [35]. For pure Zn_2SnO_4 products, the relative percentage of O_c was about 27.4%, which was lower than the proportion in PdO-loaded samples of 34.3%. The results indicate that the loading of PdO would increase the chemisorbed oxygen molecules, and maybe contribute to a good gas sensing performance as sensing material.

The morphology and microstructures of the obtained pure and 2 wt% PdO-loaded Zn_2SnO_4 products were observed by FESEM and TEM. Fig. 4a–f depicts a typical morphology of the two as-prepared Zn_2SnO_4 octahedrons. As can be seen in Fig. 4a and b, the two Zn_2SnO_4 octahedron products had a good dispersity and uniformity. Fig. 4c and d shows a single octahedron of the pure and 2 wt% PdO-loaded Zn_2SnO_4 products, respectively. It is found that the surface of the octahedrons was rough and decorated with nanosheets and it worth noting that the PdO loading treatment has no influence on the surface morphology. Fig. 4e and f display the detailed information on the surface of the two samples, which were marked with red rectangular in Fig. 4c and d, respectively. It can be seen from Fig. 4e that the nanosheets were uniformly grown on the surface of Zn_2SnO_4 octahedron, and the thickness and length of the nanosheets was uniform. Fig. 4f displays the same surface morphology as Fig. 4e. From Fig. 4e and f, it can be observed that the nanosheets were grown nearly perpendicular to the surface of Zn_2SnO_4 octahedron. Also, as can be observed the thickness and

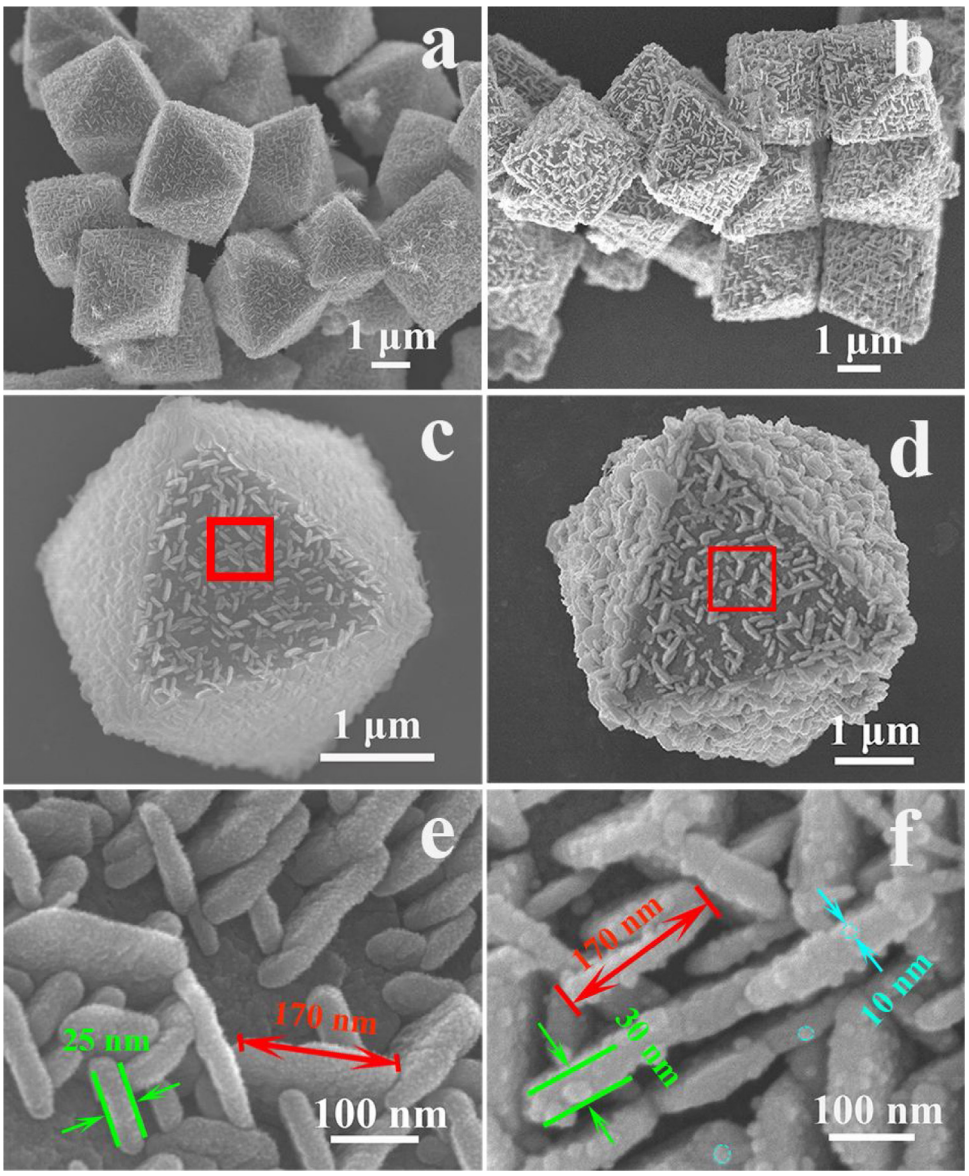

Fig. 4. (a, c and e) FESEM images of pure Zn_2SnO_4 and (b, d and f) 2wt%-PdO-loaded Zn_2SnO_4 octahedrons.

length which was marked from Fig. 4e and f that the nanosheets have a thickness and length of 20–30 nm and 150–200 nm, respectively. However, it can be also found in Fig. 4f that there are some nanoparticles uniformly dispersed on the nanosheets and the diameter of the nanoparticles was about 10 nm (as marked in Fig. 4f). These nanoparticles can be concluded to be PdO nanoparticles, which will be confirmed later.

TEM and HRTEM were utilized to further demonstrate the structure of the 2 wt% PdO-loaded Zn_2SnO_4 sample. As shown in Fig. 5a and b it can be seen that the shape and morphology of the products were matched well with those of the FESEM observations. Fig. 5c presents the magnified TEM image marked with red rectangle in Fig. 5b, it can be observed that there are some nanoparticles grown on the nanosheets. The inset of Fig. 5c displays that the size of the nanoparticles was about 10 nm, which can be speculated as PdO nanoparticles. Fig. 5d and f depicts the HRTEM images of the selected area marked with red rectangle in Fig. 5e. The clear fringe spacing of 0.26 nm observed in Fig. 5d was corresponding to the (311) plane of Zn_2SnO_4 sample. The HRTEM image shows in Fig. 5f reveal a clear lattice fringe with lattice spacing of 0.215 nm was in good agreement with the (110) plane of PdO. In order to further demonstrate the existence PdO, SAED was measured as shown in Fig. S1. TEM elemental mapping was also conducted to study the elemental distribution of the 2 wt% PdO-loaded Zn_2SnO_4 sample. The elemental mapping images corresponding to a single Zn_2SnO_4 octahedron (Fig. 5g) shown in Fig. 5h–k indicates the spatial distributions of Zn, O, Sn and Pd. It was found that the Zn, O, and Sn were homogeneously dispersed, and the PdO nanoparticles were loaded uniformly on the surface of the Zn_2SnO_4 octahedron.

3.2. Gas sensing characteristics

The gas sensing properties of the gas sensor based on unloaded and PdO-loaded Zn_2SnO_4 samples were systematically investigated. It is well known that the operating temperature plays an important role in determining the gas sensing properties owing to its impact on surface state of sensing material, as well as the interaction between the absorbed oxygen and sensing materials. In order to determine the optimum operating temperature, the response of the sensors based on pure Zn_2SnO_4 and 1 wt%, 2 wt% and 4 wt% PdO-laded Zn_2SnO_4 to 100 ppm ethanol was tested as a function of operating temperature. Fig. 6 displays the response of the four

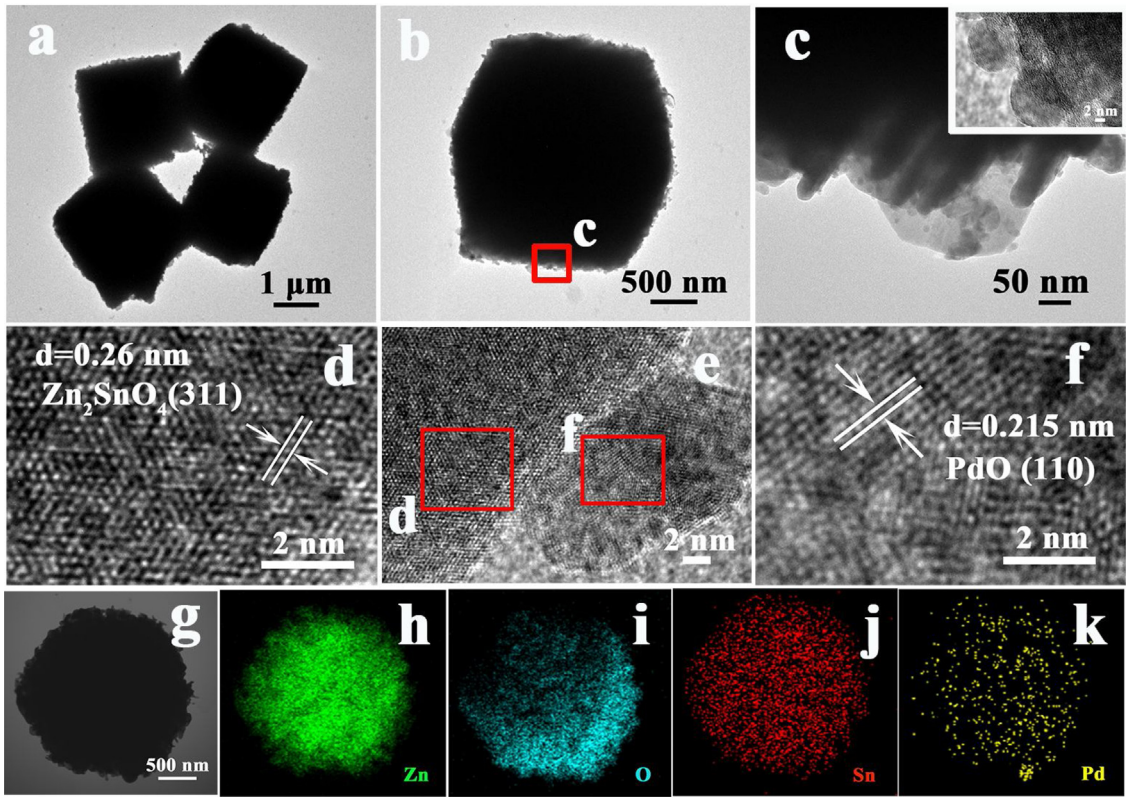

Fig. 5. (a–c) TEM images of 2wt%-PdO-loaded Zn_2SnO_4 octahedrons. (d–f) HRTEM images of as-prepared 2wt%-PdO-loaded Zn_2SnO_4 octahedrons. (g–k) TEM image of an individual microsphere and the corresponding elemental mapping images.

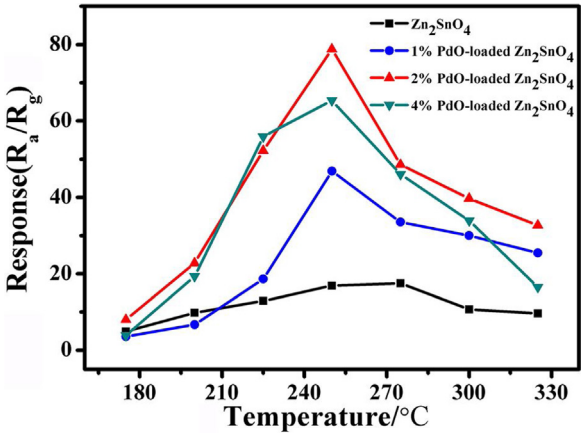

Fig. 6. Response of pure Zn_2SnO_4 and 1 wt%, 2 wt% and 4 wt% PdO-loaded Zn_2SnO_4 to 100 ppm ethanol as a function of operating temperature.

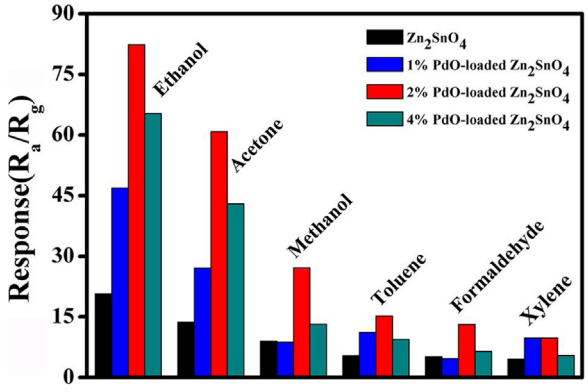

Fig. 7. Selectivity measurements of pure Zn_2SnO_4 and 1 wt%, 2 wt% and 4 wt% PdO-loaded Zn_2SnO_4 to various test gas with concentrations of 100 ppm.

sensors to 100 ppm ethanol at operating temperature from 180 to 330 °C. It is obvious that the response of the four sensors varied with the operating temperature. The response increased with a raise of operating temperature and reached the maximum value, and then decreased with further increasing temperature. Among them, the sensor based on pure Zn_2SnO_4 samples reached the maximum response value of 17.5 at 270 °C, while for the sensors based on PdO-loaded Zn_2SnO_4, the optimum operating temperature reached at 250 °C with maximum response values of 46.9 (1 wt% PdO), 82.3 (2 wt% PdO) and 65.3 (4 wt% PdO), respectively. Obviously, the sensor based on 2 wt% PdO-loaded Zn_2SnO_4 products possesses the highest ethanol response, which is almost five times higher than that of the pure Zn_2SnO_4. Compared with pure Zn_2SnO_4, the sensors based on PdO-loaded Zn_2SnO_4 showed an enhanced response and a lower operating temperature toward ethanol. The possible reason for the enhancement of the sensor is ascribed to the catalytic effect of PdO, which efficiently activates the dissociation of gas molecules at different temperature [36].

Since selectivity is a remarkable aspect of sensing properties, the response of the above four sensors toward various kinds of test gases with concentrations of 100 ppm were investigated at their optimum temperature (270 °C for pure Zn_2SnO_4, 250 °C for 1–4 wt% PdO-loaded Zn_2SnO_4), respectivety. Fig. 7 shows a bar graph of the responses of the sensors to volatile gases of ethanol, acetone, methanol, toluene, formaldehyde, and xylene. The results indicated that all the sensors showed selectivity toward ethanol as opposed to other test gases. In addition, it is worth noting that the sensor based on 2 wt% PdO-loaded Zn_2SnO_4 showed better sensing response compared with other sensors and the highest response to ethanol was 82.3. The results indicated that the introduction of

Table 1
Comparison of different ethanol gas sensors based on Zn_2SnO_4.

Sensing material	Morphology	Tem. (°C)	Con. (ppm)	Res. (Ra/Rg)	Ref.
La_2O_3-Zn_2SnO_4	Hollow fibre	200	200	52	[37]
NiO-Zn_2SnO_4	Hollow cube	280	100	52.7	[38]
Zn_2SnO_4	Octahedral-like	300	500	10	[39]
Zn_2SnO_4	Flower-like	380	100	30.8	[40]
Zn_2SnO_4	Quasi-cubic	325	600	94.3	[41]
Zn_2SnO_4	Nanowire	500	100	60.8	[42]
PdO-Zn_2SnO_4	Octahedral	250	100	82.3	This work

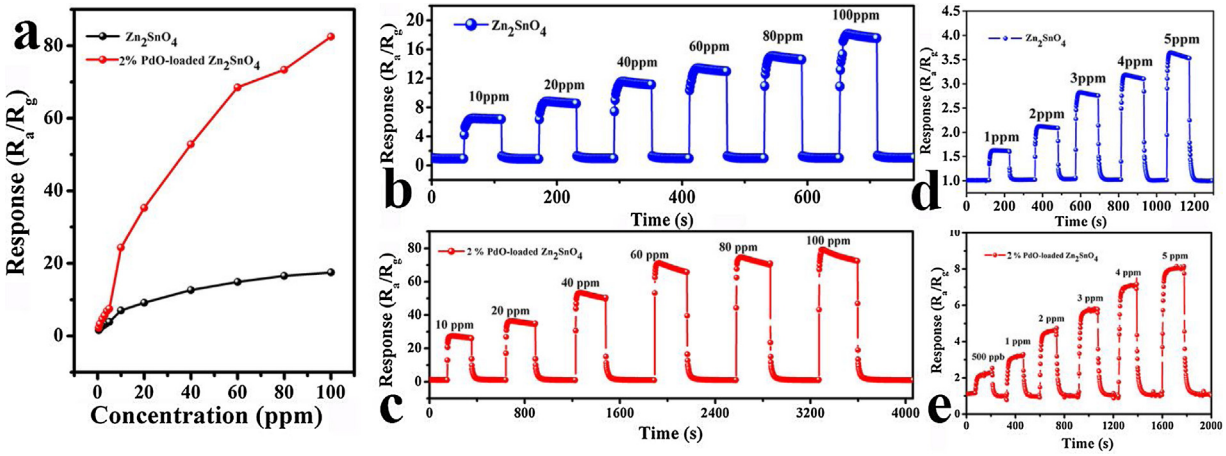

Fig. 8. (a) Response of the sensor based on pure Zn_2SnO_4 and 2 wt% PdO-loaded Zn_2SnO_4 at different concentrations at 270 °C and 250 °C. (b–e) Dynamic response curves of pure Zn_2SnO_4 and 2 wt% PdO-loaded Zn_2SnO_4 to different concentrations of ethanol at 270 °C and 250 °C.

PdO could significantly enhance the sensing response to ethanol. Based on the above experimental results the PdO-Zn_2SnO_4 composite exhibit selectivity toward ethanol, according to the literature, many factors can affect the gas sensing selectivity, such as the LUMO (lowest unoccupied molecule orbit) energy of gas molecule and the amount of gas adsorption on the sensing material at different operating temperature. A lower LUMO energy will reduce the energy needed for gas sensing reaction. Moreover, the electron affinity is affected by the orbital energy of the gas molecule, if the value of LUMO energy is lower, the gas molecule ability in capturing electrons will be stronger. Therefore, at the operating temperature of 250 °C, due to the LUMO energy of ethanol is lower than other test gas, the ability of capturing electrons will be stronger than other test gases, and therefore the sensor will exhibit higher response to ethanol [37]. In order to demonstrate the excellent sensitivity of 2 wt% PdO-Zn_2SnO_4, the sensing performance comparison between different sensors in reported literature and our present work was made. As illustrated in Table 1 [38–43], apparently, the PdO loaded Zn_2SnO_4 octahedral material exhibited much higher response at a relatively lower operating temperature than the others.

Fig. 8b and c exhibits the response behaviors of sensors based on pure Zn_2SnO_4 and 2 wt% PdO-loaded Zn_2SnO_4 to different concentrations of ethanol at optimum operating temperature of 270 °C and 250 °C, respectively. Obviously the gas response of the two sensors both exhibits a stepwise increase with the increasing of ethanol concentration from 10 to 100 ppm. The gas sensor based on 2 wt% PdO-loaded Zn_2SnO_4 composites displayed quite enhanced response. Moreover, from Fig. 8a the corresponding gas response values of the sensor based on pure Zn_2SnO_4 were merely 7.0, 9.1, 12.6, 14.9, 16.4 and 17.5, while for the sensor based on 2 wt% PdO-loaded Zn_2SnO_4, the response values were 24.4, 35.3, 52.8, 68.5, 73.4 and 82.3. With the concentration of ethanol added up to 60 ppm, the response of sensor based on pure Zn_2SnO_4 nearly had no prominent increase. However, the responses of sensor based on 2 wt% PdO-loaded Zn_2SnO_4 depended near linearly on the gas concentration. In addition, from Fig. 8d and e, it is evidently displays that the ethanol response of the two sensors increased step by step during the concentration from 1 to 5 ppm. The response of the sensor based on PdO-loaded Zn_2SnO_4 displayed quite enhanced gas sensing characteristics, and the detection limit can be as low as 500 ppb. It can be concluded that the PdO loading could significantly decrease the detection limit.

Fig. 9a–d displays the responses of 2 wt% PdO-loaded Zn_2SnO_4 to 100 ppm ethanol at 250 °C. It can be obviously observed from Fig. 9b and c that the response time (τ_{res}) of the sensor toward ethanol was as low as 1s, while the recovery time (τ_{recov}) toward ethanol was 206 s. Clearly, the sensor showed a relatively rapid response to ethanol, while the recovery time was a little bit long. Moreover, the five reversible cycles of response and recovery curves of the sensor to 100 ppm ethanol shown in Fig. 9d reveals that the sensor possesses a stable and repeatable sensing property.

3.3. Gas sensing machenism

For the sensing mechanism of semiconductor oxides, the widely accepted theory is based on the space charge model, which is based on the change in resistance of the sensor upon exposed to different gas atmospheres [44–46]. The gas sensing mechanism can be considered as the following, as illustrated in Fig. 10a: when the sensor is exposed to ambient air, oxygen molecules (O_2) absorb on the surface of the sensing material, and form surface-absorbed oxygen species ($O_2^-{}_{(ads)}$, $O^-{}_{(ads)}$, $O^{2-}{}_{(ads)}$) by capturing free electrons from the conduction band of the sensing material, and formed a depletion layer at the surface of Zn_2SnO_4 octahedrons. In this process, oxygen molecules act as electron acceptors, which result in the decrease of electrons concentration and increase the resistance of the sensor. When the sensor is exposed to reducing gases, for instance, ethanol and acetone at a moderate temperature, these gas molecules will react with the absorbed oxygen species (Eqs. (1)–(3)). This process release the trapped electrons back into the

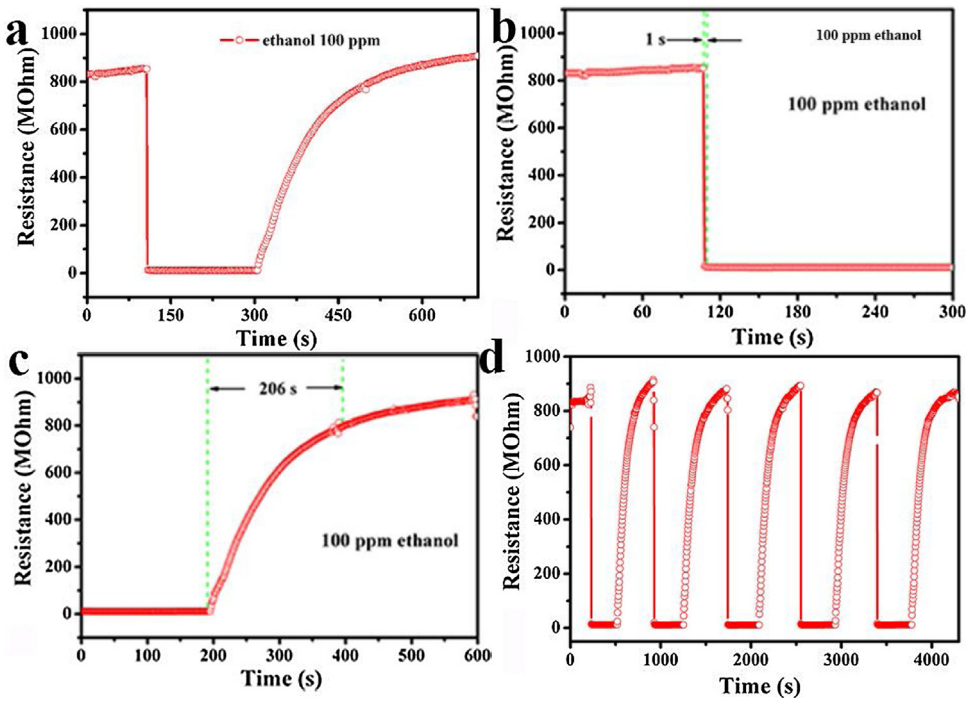

Fig. 9. (a) Response transients of 2 wt% PdO-loaded Zn_2SnO_4 to ethanol and acetone with concentration of 100 ppm at 250 °C. (b and c)The dynamic response and recovery curve of the sensor based on 2 wt% PdO-loaded Zn_2SnO_4 to 100 ppm ethanol at 250 °C. (d and e) Five periods of response and recovery curve to 100 ppm acetone and ethanol respectively.

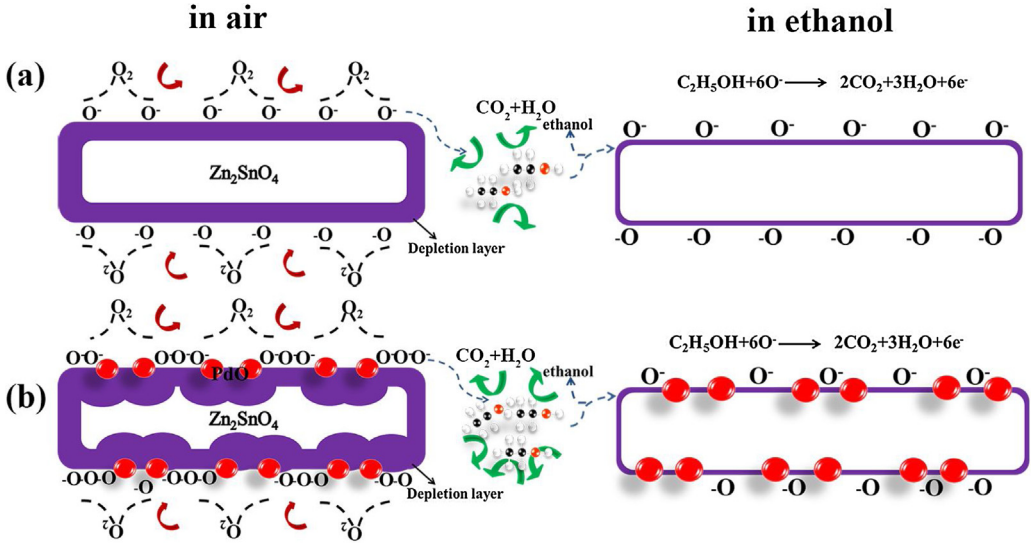

Fig. 10. Schematic diagram of the gas sensing mechanism (a) Zn_2SnO_4 (b) PdO-loaded Zn_2SnO_4.

conduction band, and lead to the increase of the conductivity, thereby lowering the measured resistance of sensor and decreasing the width of the surface depletion layer.

$$C_2H_5OH + 6O^-_{(ads)} \quad 2CO_{2+}3H_2O + 6e^- \tag{1}$$

$$C_3H_6O + 8O^-_{(ads)} \quad 3CO_2 + 3H_2O + 8e^- \tag{2}$$

$$CH_3OH + 3O^-_{(ads)} \quad CO_{2+}2H_2O + 3e^- \tag{3}$$

It has been clearly revealed that the introduction of PdO could significantly enhanced the gas sensing performance, indicating that the decorating of PdO nanoparticles contributed greatly to the improvement of sensing properties. The high response of PdO loaded Zn_2SnO_4 is possibly related to electronic as well as chemical sensitization of PdO nanoparticles. As illustrated in Fig. 10a and b, in electronic sensitization, electrons will transfer from *n*-type semiconductor oxides to PdO nanoparticles as the work function of PdO (~7.9 eV) [47] is higher than Zn_2SnO_4 (4.81 eV) [48], this will result in extending of electron depletion layer and increasing of resistance of PdO-Zn_2SnO_4 in air. In chemical sensitization, PdO nanoparticles would catalytically activate the dissociation of oxygen molecules and promote the gas sensing reactions through enhancement of the adsorption and dissociation of analyte gases [49,50]. Under the catalytic effect of PdO, the molecule-ion conversion rate and the quantity of adsorbed oxygen ions can be greatly increased, resulting in the greater and faster degree of electron depletion of Pd-loaded Zn_2SnO_4 octahedrons, as illustrated in Fig. 10b. Therefore, the sensing performance of PdO-loaded Zn_2SnO_4 is obviously higher than that of pristine Zn_2SnO_4. Moreover, PdO-loading as an

efficient method for improving gas sensing properties have been demonstrated [51–53].

4. Conclusions

In summary, we developed a facile method for the preparation of PdO functionalized Zn_2SnO_4 octahedron composites. The surface of Zn_2SnO_4 octahedrons are decorated with nanosheets. A comparative gas sensing investigation between pure Zn_2SnO_4 and PdO-loaded Zn_2SnO_4 was carried out, and the results demonstrated that of all the tested sensors, the 2 wt% PdO-loaded Zn_2SnO_4 exhibited the highest sensitivity. The response to ethanol was 82.5, which was about five times higher than pristine Zn_2SnO_4. The enhancement of the sensing properties was attributed to the unique architecture of the Zn_2SnO_4 octahedral products as well as the catalytic effect of PdO.

Acknowledgements

This work is supported by the National Key Research and Development Program of China (No. 2016YFC0207300). National Nature Science Foundation of China (Nos. 61503148, 61520106003, 61327804). National High-Tech Research and Development Program of China (863 Program, No. 2014AA06A505). Science and Technology Development Program of Jilin Province (No. 20170520162JH). China Postdoctoral Science Foundationfunded project No. 2015M580247.

Appendix A. Supplementary data

Supplementary data associated with this article can be found, in the online version, at https://doi.org/10.1016/j.snb.2018.03.121.

References

[1] D.R. Miller, S.A. Akbar, P.A. Morris, Nanoscale metal oxide-based heterojunctions for gas sensing: a review, Sens. Actuators B: Chem. 204 (2014) 250–272.
[2] N. Yamazoe, Toward innovations of gas sensor technology, Sens. Actuators B: Chem. 108 (2005) 2–14.
[3] Y. Shimizu, M. Egashira, Basic aspects and challenges of semiconductor gas sensors, MRS Bull. 24 (1999) 18–24.
[4] P. Sun, L. You, D. Wang, Y. Sun, J. Ma, G. Lu, Synthesis and gas sensing properties of bundle-like alpha-Fe2O_3 nanorods, Sens. Actuators B: Chem. 156 (2011) 368–374.
[5] K. Tian, X.-X. Wang, Z.-Y. Yu, H.-Y. Li, X. Guo, Hierarchical and hollow Fe_2O_3 nanoboxes derived from metal-organic frameworks with excellent sensitivity to H_2S, ACS Appl. Mater. Interfaces 9 (2017) 29669–29676.
[6] N. Barsan, M. Schweizer-Berberich, W. Gopel, Fundamental and practical aspects in the design of nanoscaled SnO_2 gas sensors: a status report, Fresenius J. Anal. Chem. 365 (1999) 287–304.
[7] J.-H. Kim, H.W. Kim, S.S. Kim, Self-heating effects on the toluene sensing of Pt-functionalized SnO_2-ZnO core-shell nanowires, Sens. Actuators B: Chem. 251 (2017) 781–794.
[8] P. Sun, Y. Cao, J. Liu, Y. Sun, J. Ma, G. Lu, Dispersive SnO_2 nanosheets: hydrothermal synthesis and gas-sensing properties, Sens. Actuators B: Chem. 156 (2011) 779–783.
[9] S.-J. Kim, I.-S. Hwang, J.-K. Choi, Y.C. Kang, J.-H. Lee, Enhanced C_2H_5OH sensing characteristics of nano-porous In_2O_3 hollow spheres prepared by sucrose-mediated hydrothermal reaction, Sens. Actuators B: Chem. 155 (2011) 512–518.
[10] S. Roso, D. Degler, E. Llobet, N. Barsan, A. Urakawa, Temperature-dependent NO_2 sensing mechanisms over indium oxide, ACS Sens. 2 (2017) 1272–1277.
[11] S. Xu, Z.L. Wang, One-dimensional ZnO nanostructures: solution growth and functional properties, Nano Res. 4 (2011) 1013–1098.
[12] Z. Liu, L. Yu, F. Guo, S. Liu, L. Qi, M. Shan, X. Fan, Facial development of high performance room temperature NO_2 gas sensors based on ZnO nanowalls decorated rGO nanosheets, Appl. Surf. Sci. 423 (2017) 721–727.
[13] Q. Wan, Q.H. Li, Y.J. Chen, T.H. Wang, X.L. He, J.P. Li, C.L. Lin, Fabrication and ethanol sensing characteristics of ZnO nanowire gas sensors, Appl. Phys. Lett. 84 (2004) 3654–3656.
[14] S. Kabcum, N. Kotchasak, D. Channei, A. Tuantranont, A. Wisitsoraat, S. Phanichphant, C. Liewhiran, Highly sensitive and selective NO_2 sensor based on Au-impregnated WO_3 nanorods, Sens. Actuators B: Chem. 252 (2017) 523–536.
[15] Y.H. Cho, Y.C. Kang, J.-H. Lee, Highly selective and sensitive detection of trimethylamine using WO_3 hollow spheres prepared by ultrasonic spray pyrolysis, Sens. Actuators B: Chem. 176 (2013) 971–977.
[16] Y. Du, W. Wang, X. Li, J. Zhao, J. Ma, Y. Liu, G. Lu, Preparation of NiO nanoparticles in microemulsion and its gas sensing performance, Mater. Lett. 68 (2012) 168–170.
[17] P. Rai, J.-W. Yoon, H.-M. Jeong, S.-J. Hwang, C.-H. Kwak, J.-H. Lee, Design of highly sensitive and selective Au@NiO yolk-shell nanoreactors for gas sensor applications, Nanoscale 6 (2014) 8292–8299.
[18] H. Gao, D. Wei, P. Lin, C. Liu, P. Sun, K. Shimanoe, N. Yamazoe, G. Lu, The design of excellent xylene gas sensor using Sn-doped NiO hierarchical nanostructure, Sens. Actuators B: Chem. 253 (2017) 1152–1162.
[19] E.L. Foletto, J.M. Simoes, M.A. Mazutti, S.L. Jahn, E.I. Muller, L.S. Fagundes Pereira, E.M. de Moraes Flores, Application of Zn_2SnO_4 photocatalyst prepared by microwave-assisted hydrothermal route in the degradation of organic pollutant under sunlight, Ceram. Int. 39 (2013) 4569–4574.
[20] M. Ben Ali, F. Barka-Bouaifel, H. Elhouichet, B. Sieber, A. Addad, L. Boussekey, M. Ferid, R. Boukherroub, Hydrothermal synthesis phase structure, optical and photocatalytic properties of Zn_2SnO_4 nanoparticles, J. Colloid Interface Sci. 457 (2015) 360–369.
[21] J. Wang, H. Li, S. Meng, L. Zhang, X. Fu, S. Chen, One-pot hydrothermal synthesis of highly efficient SnOx/Zn_2SnO_4 composite photocatalyst for the degradation of methyl orange and gaseous benzene, Appl. Catal. B 200 (2017) 19–30.
[22] B. Tan, E. Toman, Y. Li, Y. Wu, Zinc stannate (Zn_2SnO_4) dye-sensitized solar cells, J. Am. Chem. Soc. 129 (2007) 4162–4163.
[23] A. Bera, A.D. Sheikh, M.A. Haque, R. Bose, E. Alarousu, O.F. Mohammed, T. Wu, Fast crystallization and improved stability of perovskite solar cells with Zn_2SnO_4 electron transporting layer: interface matters, ACS Appl. Mater. Interfaces 7 (2015) 28404–28411.
[24] W.-Q. Wu, D. Chen, R.A. Caruso, Y.-B. Cheng, Recent progress in hybrid perovskite solar cells based on n-type materials, J. Mater. Chem. A 5 (2017) 10092–10109.
[25] A. Rong, X.P. Gao, G.R. Li, T.Y. Yan, H.Y. Zhu, J.Q. Qu, D.Y. Song, Hydrothermal synthesis of Zn_2SnO_4 as anode materials for Li-ion battery, J. Phys. Chem. B 110 (2006) 14754–14760.
[26] C.T. Cherian, M. Zheng, M.V. Reddy, B.V.R. Chowdari, C.H. Sow, Zn_2SnO_4 nanowires versus nanoplates: electrochemical performance and morphological evolution during Li-cycling, ACS Appl. Mater. Interfaces 5 (2013) 6054–6060.
[27] S. Sun, S. Liang, Morphological zinc stannate: synthesis, fundamental properties and applications, J. Mater. Chem. A 5 (2017) 20534–20560.
[28] X.-G. Han, X.-W. Cao, L. Li, C. Wang, Fabrication and characterization of polliwog-like Sn/Zn_2SnO_4 heterostructure nanocrystal and their gas sensing properties, Sens. Actuators B: Chem. 185 (2013) 383–388.
[29] Q. Zhao, D. Ju, X. Song, X. Deng, M. Ding, X. Xu, H. Zeng, Polyhedral Zn_2SnO_4: Synthesis, enhanced gas sensing and photocatalytic performance, Sens. Actuators B: Chem. 229 (2016) 627–634.
[30] Z. Lu, Y. Tang, Two-step synthesis and ethanol sensing properties of Zn_2SnO_4-SnO_2 nanocomposites, Mater. Chem. Phys. 92 (2005) 5–9.
[31] Y.-Q. Jiang, C.-X. He, R. Sun, Z.-X. Xie, L.-S. Zheng, Synthesis of Zn_2SnO_4 nanoplate-built hierarchical cube-like structures with enhanced gas-sensing property, Mater. Chem. Phys. 136 (2012) 698–704.
[32] Z. Chen, M. Cao, C. Hu, Novel Zn_2SnO_4 Hierarchical nanostructures and their gas sensing properties toward ethanol, J. Phys. Chem. C 115 (2011) 5522–5529.
[33] H.M. Yang, S.Y. Ma, H.Y. Jiao, Q. Chen, Y. Lu, W.X. Jin, W.Q. Li, T.T. Wang, X.H. Jiang, Z. Qiang, H. Chen, Synthesis of Zn_2SnO_4 hollow spheres by a template route for high-performance acetone gas sensor, Sens. Actuators B: Chem. 245 (2017) 493–506.
[34] W.-T. Koo, S.-J. Choi, S.-J. Kim, J.-S. Jang, H.L. Tuller, I.-D. Kim, Heterogeneous sensitization of metal-organic framework driven metal@metal oxide complex catalysts on an oxide nanofiber scaffold toward superior gas sensors, J. Am. Chem. Soc. 138 (2016) 13431–13437.
[35] J.C. Dupin, D. Gonbeau, P. Vinatier, A. Levasseur, Systematic XPS studies of metal oxides, hydroxides and peroxides, Phys. Chem. Chem. Phys. 2 (2000) 1319–1324.
[36] N. Ma, K. Suematsu, M. Yuasa, T. Kida, K. Shimanoe, Effect of water vapor on Pd-loaded SnO_2 nanoparticles gas sensor, ACS Appl. Mater. Interfaces 7 (2015) 5863–5869.
[37] Z. Wen, L. Tian-mo, Gas-sensing properties of SnO_2-TiO_2-based sensor for volatile organic compound gas and its sensing mechanism, Phys. B-Condens. Matter 405 (2010) 1345–1348.
[38] H.M. Yang, S.Y. Ma, G.J. Yang, Q. Chen, Q.Z. Zeng, Q. Ge, L. Ma, Y. Tie, Synthesis of La_2O_3 doped Zn_2SnO_4 hollow fibers by electrospinning method and application in detecting of acetone, Appl. Surf. Sci. 425 (2017) 585–593.
[39] S. Zhang, G. Sun, Y. Li, B. Zhang, L. Lin, Y. Wang, J. Cao, Z. Zhang, Continuously improved gas-sensing performance of SnO_2/Zn_2SnO_4 porous cubes by structure evolution and further NiO decoration, Sens. Actuators B: Chem. 255 (2018) 2936–2943.
[40] Z.G. Lu, Y.G. Tang, Two-step synthesis and ethanol sensing properties of Zn2SnO4-SnO2 nanocomposites, Mater. Chem. Phys. 92 (2005) 5–9.
[41] C. Chen, G. Li, J. Li, Y. Liu, One-step synthesis of 3D flower-like Zn_2SnO_4 hierarchical nanostructures and their gas sensing properties, Ceram. Int. 41 (2015) 1857–1862.

[42] Y.-Q. Jiang, X.-X. Chen, R. Sun, Z. Xiong, L.-S. Zheng, Hydrothermal syntheses and gas sensing properties of cubic and quasi-cubic Zn_2SnO_4, Mater. Chem. Phys. 129 (2011) 53–61.
[43] T. Tharsika, A.S.M.A. Haseeb, S.A. Akbar, M.F.M. Sabri, Y.H. Wong, Gas sensing properties of zinc stannate ($Zn_2SnO_{4)}$ nanowires prepared by carbon, assisted thermal evaporation process, J. Alloys Compd. 618 (2015) 455–462.
[44] R.W.J. Scott, S.M. Yang, G. Chabanis, N. Coombs, D.E. Williams, G.A. Ozin, Tin dioxide opals and inverted opals: near-ideal microstructures for gas sensors, Adv. Mater. 13 (2001) 1468-.
[45] H. Ogawa, M. Nishikawa, A. Abe, Hall measurement studies and an electrical conduction model of tin oxide ultrafine particle films, J. Appl. Phys. 53 (1982) 4448–4455.
[46] D.-J. Yang, I. Kamienchick, D.Y. Youn, A. Rothschild, I.-D. Kim, Ultrasensitive and highly selective gas sensors based on electrospun SnO_2 nanofibers modified by Pd loading, Adv. Funct. Mater. 20 (2010) 4258–4264.
[47] J. Rogal, K. Reuter, M. Scheffler, Thermodynamic stability of PdO surfaces, Phys. Rev. B 69 (2004).
[48] X.-Y. Liu, H.-W. Zheng, Z.-L. Zhang, X.-S. Liu, R.-Q. Wan, W.-F. Zhang, Effect of energy level matching on the enhancement of photovoltaic response about oxide/Zn_2SnO_4 composites, J. Mater. Chem. 21 (2011) 4108–4116.
[49] A. Kolmakov, D.O. Klenov, Y. Lilach, S. Stemmer, M. Moskovits, Enhanced gas sensing by individual SnO_2 nanowires and nanobelts functionalized with Pd catalyst particles, Nano Lett. 5 (2005) 667–673.
[50] M. Zhao, J.X. Huang, C.W. Ong, Diffusion-controlled H_2 sensors composed of Pd-coated highly porous WO3 nanocluster films, Sens. Actuators B: Chem. 191 (2014) 711–718.
[51] Y. Zeng, Z. Lou, L. Wang, B. Zou, T. Zhang, W. Zheng, G. Zou, Enhanced ammonia sensing performances of Pd-sensitized flowerlike ZnO nanostructure, Sens. Actuators B: Chem. 156 (2011) 395–400.
[52] Y.-J. Chiang, F.-M. Pan, PdO nanoflake thin films for CO gas sensing at low temperatures, J. Phys. Chem. C 117 (2013) 15593–15601.
[53] S.-W. Choi, S.S. Kim, Room temperature CO sensing of selectively grown networked ZnO nanowires by Pd nanodot functionalization, Sens. Actuators B: Chem. 168 (2012) 8–13.

Biographies

Xueli Yang received her B. Eng. degree in 2013 and M.S. degree in 2016 from College of Science, Northeast Forestry University in China. Currently she is studying for her Ph.D. degree in College of Electronic Science and Engineering, Jilin University, China.

Hongyu Gao received the BS degree in Department of Electronic Science and Engineering in 2016. He is currently studying for his MS degree in College of Electronic Science and Engineering, Jilin University, China.

Liupeng Zhao received the B. Eng. degree in department of electronic sciences and technology, Jilin University, in 2016. At the same year, he entered his MS course in College of Electronic Science. Now, he is studying for his MS degree, majored in the synthesis and characterization of the semiconducting functional materials and gas sensors.

Tianshuang Wang He is currently working toward the MS degree in the Electronics Science and Engineering department, Jilin University. His research interests include the synthesis of functional materials and their applications in gas sensors.

PengSun received his PhD degree from College of Electronic Science and Engineering, Jilin University, China in 2014. He was appointed the lecturer in Jilin University in the same year. Now, he is engaged in the synthesis and characterization of the semiconducting functional materials and gas sensors.

Fangmeng Liu received his PhD degree in 2017 from College of Electronic Science and Engineering, Jilin University, China. Now he is a lecturer of Jilin University, China. His current research interests include the application of functional materials and development of solid state electrolyte gas sensor and flexible device.

Geyu Lu received the B.Sci. degree in electronic sciences in 1985 and the M.S.degree in 1988 from Jilin University in China and the Dr. Eng. degree in 1998 from Kyushu University in Japan. Now he is a professor of Jilin University, China. His current research interests include the development of chemical sensors and the application of the function materials.